PDGF-BB carried by endothelial Cell-derived extracellular vesicles reduces vascular smooth muscle cell apoptosis in diabetes

PDGF-BB carried by endothelial cell-derived extracellular vesicles reduces vascular smooth muscle cell apoptosis in diabetes

Gabriele Togliatto[1], Patrizia Dentelli[1], Arturo Rosso[1], Giusy Lombardo[1], Maddalena Gili[1], Sara Gallo[1], Chiara Gai[1], Anna Solini[2], Giovanni Camussi[1*], Maria Felice Brizzi[1*]

[1]Department of Medical Sciences, University of Torino, Italy

[2]Department of Surgical, Medical, Molecular and Critical Area Pathology, University of Pisa, Italy

GT and PD equally contributed

[*]**Address correspondence to:**

Maria Felice Brizzi and Giovanni Camussi, Department of Medical Sciences, University of Turin, Corso Dogliotti 14, 10126, Turin

mariafelice.brizzi@unito.it

giovanni.camussi@unito.it

Abstract words: 200

Main text words: 3906

Number of tables/figures: 8

Running Title: mbPDGF-BB in CD31EVs and vascular smooth muscle cell apoptosis

Key words: miR-296-5p, PDGF-BB, extracellular vesicles, diabetes, vascular smooth muscle cells.

ABSTRACT

Endothelial cell-derived extracellular vesicles (CD31EVs) are a new entity for therapeutic/prognostic purposes. The roles of CD31EVs as mediators of smooth muscle cell (VSMC) dysfunction in type 2 diabetes (T2D) is investigated herein.

We demonstrated that, unlike non-diabetic, diabetic serum-derived-EVs (D-CD31EVs) boosted apoptosis resistance of VSMCs cultured in hyperglycaemic condition. Biochemical analysis revealed that this effect relies on changes in the balance between anti-apoptotic/pro-apoptotic signals: increase of bcl-2 and decrease of bak/bax. D-CD31EV cargo analysis demonstrated that D-CD31EVs are enriched in membrane-bound-platelet-derived-growth-factor-BB (mbPDGF-BB). Thus, we postulated that mbPDGF-BB transfer by D-CD31EVs could account for VSMC resistance to apoptosis. By depleting CD31EVs of PDGF-BB or blocking the PDGF-BB-receptorβ on VSMCs, we demonstrated that mbPDGF-BB contributes to D-CD31EV-mediated bak/bax and bcl-2 levels. Moreover, we found that bak expression is under the control of PDGF-BB-mediated miR-296-5p expression. In fact, while PDGF-BB-treatment recapitulated D-CD31EV-mediated anti-apoptotic program and VSMC resistance to apoptosis, PDGF-BB-depleted CD31EVs failed. D-CD31EVs also increased VSMC migration and recruitment to neovessels, by means of PDGF-BB. Finally, we found that VSMCs, from human atherosclerotic arteries of T2D individuals, express low bak/bax and high bcl-2 and miR-296-5p levels. This study identifies the mbPDGF-BB in D-CD31EVs as a relevant mediator of diabetes-associated VSMC resistance to apoptosis.

INTRODUCTION

Cardiovascular complications are a leading cause of morbidity and premature mortality in diabetes (1,2). Structural alterations to vessel walls result in intima-media thickening which marks individuals at high risk to develop acute cardiovascular events (3,4). Moreover, restenosis is still a major complication in the diabetic setting. A main cause of re-occlusion is intimal hyperplasia which is due to the migration and/or excessive growth of vascular smooth muscle cells (VSMCs). A dysregulated balance between apoptosis and the proliferation of VSMCs seems to play a crucial role in intima-media thickening in diabetic individuals (5,6). Indeed, *in vitro* studies have suggested that high glucose (HG) induces the expression of bcl-2 family members and inhibits the apoptotic protein Inhibitor of Apoptosis Protein 1, (IAP-1) in VSMCs (7). In addition, Ruiz *et al.* (8) have demonstrated that VSMCs, recovered from diabetic patients, showed a resistance to apoptosis which was possibly due to bcl-2 over-expression. Although circulating high glucose concentration might *per se* induce VSMC dysfunction, additional events can contribute to this process *in vivo*.

Several studies have focused on extracellular RNA (exRNA) transporters, indicating that they may be present in biological fluids in the form of vesicles, which have been denoted microvesicles, exosomes, membrane particles and apoptotic bodies (9,10). Despite the lack of consensus on vesicle classification, the presence of overlapping characteristics and biological activity has evoked the use of the inclusive term; “extracellular vesicles” (EVs) (11,12). The paracrine/endocrine effects of EVs have recently gained significant attention (13,14). Indeed, EV biological activity has been linked to the transfer of bioactive molecules, including proteins and microRNA (miRs) (10-14). EVs are widely distributed in human body fluids, while circulating EV cargo usually reflects the cell of origin in its physiological and/or pathological condition (9-15). Indeed, the number and cargo of circulating EVs have been suggested as a means to predict the presence of disease and even the risk of developing disease (16,17).

Increased levels of circulating platelet- and endothelial cell- (EC) derived microparticles have been proposed as “biomarkers” of cell dysfunction (18,19). However, EVs might also deliver specific drivers of disease, as they behave as diffusible vectors of biological activity and participate in exchanging information. This study therefore investigates the role of EC-derived EVs as mediators of VSMC fate in type 2 diabetes (T2D).

RESEARCH DESIGN AND METHODS

Reagents and antibodies are reported in Supplemental Table 1.

Patients and Controls. 11 T2D and 6 non-diabetic individuals (controls), who had undergone carotid endoarteriectomy surgery in our clinic, were included in the study. Clinical characteristics are reported in Supplemental Table 2. All diabetic individuals were under statin and metformin treatment. Ethical approval was obtained from Azienda Ospedaliero-Universitaria (AOU), Città della Salute e della Scienza di Torino, Italy. Informed consent was obtained from all individuals in accordance with the Declaration of Helsinki. We had no direct contact with the participants.

Isolation of VSMCs from human atherosclerotic plaque specimens. Human atherosclerotic plaque specimens were recovered from the above reported subjects (T2D: D; non-diabetic: ND) and processed as previously described (20). Vascular tissue was rinsed 3 times with phosphate-buffered saline (PBS) and intima was removed in order to furnish the VSMCs. Tunica media were finely cut into 2-3 mm pieces and subjected to enzymatic digestion using collagenase type I (0.1mg/ml) in a Dulbecco's Modified Eagle Medium (DMEM) for 1.5h at 37°C. Digestion media were collected and filtered through nylon mesh cell strainers (100μm) to remove the undigested explants. The resulting supernatants were centrifuged at 1200 rpm for 10 min and cells were plated at 2.5×10^4 cells/cm^2 and cultured with Modified Eagle Medium (MEM) supplemented with 20% (v/v) foetal bovine serum (FBS), 1% penicillin-streptomycin. Fluorescence-activated cell sorting (FACS) analysis was performed on D-VSMCs and ND-VSMCs to characterize them, as indicated in (20), using antibodies directed to CD31 and alpha-smooth muscle actin (α-SMA), directly or indirectly conjugated with fluorescein isothiocyanate (FITC) fluorochrome. FITC mouse non-immune isotypic IgG (BD Bioscience Pharmingen) was used as control.

Cell cultures. Primary macrovascular endothelial cells (ECs) and VSMCs were purchased from Lonza (Basel, Switzerland) and cultured as described by the manufacturer's instructions. VSMCs and

ECs were used at II-III cell-culture passage. To collect the EVs, ECs were starved under either low (LG, 5mmol/l) or high glucose (HG, 25 mmol/l) and 24h deprived of bovine calf serum (BCS). Cell viability was evaluated. siRNA technology was also performed in HG-cultured ECs using siRNA negative control or the Platelet-Derived Growth Factor (PDGF-BB) siRNA (Applied Biosystems) (21). EV isolation was obtained from HG-cultured ECs depleted of PDGF-BB. In selected experiments, VSMCs were cultured in LG or HG and then treated in the presence of ND-CD31EVs, D-CD31EVs or EC-derived-EVs (5×10^3 EVs/target cell), or stimulated with PDGF-BB. In selected experiments, HG-cultured VSMCs were pre-incubated with a blocking PDGF-Receptor-β (PDGFRβ) antibody (5μg/ml). Details are reported in Supplemental Materials. All experiments were performed in accordance with European Guidelines and policies and approved by the Ethical Committee of the University of Turin.

Isolation and characterization of CD31EVs from sera of T2D and non-diabetic individuals. Human serum from all above T2D and non-diabetic individuals was obtained before surgery and after informed consent. EVs from each participant were obtained by centrifuging serum as previously described (22). The supernatant was subsequently submitted to differential ultracentrifugation at 10k and 100k g for 2h at 4°C. EV pellets were then re-suspended in DMEM and stored at -80°C. FACS analysis of D-EVs and ND-EVs was performed as indicated in (23), using anti-CD31-allophycocyanin (APC), anti-CD14-phycoerythrin (PE) and anti-CD42b-FITC antibodies. FITC, PE or APC mouse non-immune isotypic IgG (BD Bioscience Pharmingen) were used as controls. FACS analysis was performed using a Guava easyCyteTM Flow Cytometer (Millipore, Germany). Fluorochrome conjugated antibodies were added to a suspension of EVs ($2.5x10^6$ particles/100 μl) for 15 min at 4°C. Surface marker expression is reported in the representative histograms as the percentage of expression±SD. The CD31 microbead kit (Miltenyi Biotec, Auburn, CA, USA) was used to isolate CD31EVs from the sera of T2D (D-CD31EVs) and non-diabetic individuals (ND-CD31EVs) (24). Briefly, 0,5 ml of freshly-thawed plasma was incubated with 100 μl of CD31

microbeads for 4h at 4°C. EVs captured on CD31 Ab-coated magnetic beads were recovered from the magnetic column (MS column) as described in the manufacturer's instructions. EV-bound beads were submitted to differential ultracentrifugation (Beckman Coulter Optima L-90K ultracentrifuge; Beckman Coulter, Fullerton, CA) for 3h at 4°C. CD31EVs were either used fresh or were stored at -80°C and then processed for transmission electron microscopy (TEM), biological effects, western blot and q-RT-PCR analysis. CD63 content in CD31EVs was analyzed by western blot. Details are reported in Supplemental Materials.

Transmission electron microscopy. TEM was performed on CD31EVs that had been isolated by ultracentrifugation and re-suspended in PBS, placed on 200 mesh nickel formvar carbon coated grids (Electron Microscopy Science, Hatfield, PA) and left to adhere for 20 min. Grids were then processed as previously described (25) and observed under a Jeol JEM 1010 electron microscope (Jeol, Tokyo, Japan). Details are reported in Supplemental Materials.

Isolation of EC-derived EVs. ECs were cultured in LG or HG DMEM without BCS for 24h, in order to collect the EVs from supernatants as previously described (21,22) and detailed in Supplemental Materials. EV number and size distribution analysis was performed using a NanoSight LM10 (NanoSight Ltd, Minton Park UK). Results were displayed as number per ml and as a frequency size distribution graph, outputted to a spreadsheet. EC-derived-EVs (LG-EVs or HG-EVs) were processed for biological, western blot and q-RT-PCR analysis (21,22).

Western blot analysis. Cells and EVs were lysed and protein concentrations were obtained, as previously described (25). Protein levels were normalized to α-SMA, β-actin, or CD63 content. Details are reported in Supplemental Materials.

EV internalization. The internalization of EVs was evaluated using confocal microscopy (LSM5-PASCAL; Zeiss, Oberkochen, Germany) as previously described (25). EV pellets were added to HG-

123 cultured VSMCs ($2x10^4$) pre-treated or not with a blocking PDGFRβ antibody. Z-stack confocal
124 microscopy VSMC images were also obtained (25). Details are reported in Supplemental Materials.

125 **RNA isolation and quantitative real-time PCR (qRT-PCR) for miRs.** Total RNA was isolated
126 from the VSMCs of atherosclerotic plaque specimens and from human VSMCs, that had been treated
127 as indicated or left untreated, using the TRIzol reagent (Invitrogen) as previously described (26).
128 RNA from cells and EVs was then reverse-transcribed using a TaqMan microRNA RT kit, specific
129 for miR-24-3p, miR-221, miR-222 and miR-296-5p, or a Syber Green microRNA RT Kit specific for
130 miR-21-5p, miR-29a and miR-145, as indicated. miR expression was normalized to the small nuclear
131 RNA, RNU6B. Loss- and gain-of-function experiments were performed in VSMCs that had been
132 transfected with the antago-miR control, the antago-miR-296-5p, pre-miR control or pre-miR-296-
133 5p oligonucleotides (Applied Biosystem), according to manufacturer's instructions (26). Details are
134 reported in Supplemental Materials.

135 **Luciferase miRNA target reporter assay.** The luciferase reporter assay was performed using a
136 construct generated by subcloning the PCR products amplified from the full-length 3'UTR of human
137 *BAK1* DNA into the Xba restriction site of the luciferase reporter vector pGL3 (Promega, Madison,
138 WI, USA). The PCR products were obtained using the primers for *BAK1* and reported in detail in
139 Supplemental Materials (26).
140 **Cell proliferation and apoptosis assay**. Proliferative activity was assayed as previously described
141 (27). For the apoptosis assay, VSMCs were subjected to Muse Annexin V and the cell dead assay
142 (Merck, Darmstadt, Germany) in accordance with manufacturer's instructions. Details are reported
143 in Supplemental Materials.

144 **Tubule-like structure formation assay**. To analyze the EC/VSMC interaction, 24-well-plates were
145 coated with growth factor-reduced Matrigel matrix (BD Biosciences) (28). Briefly, HG-cultured ECs
146 and VSMCs were pre-treated, for 24h, with either D-CD31EVs, ND-CD31EVs or HG-EVs that had
147 either been depleted, or not, of PDGF-BB. $4.5x10^4$ red labeled ECs (PKH26 vital dye) were placed

in HG medium on top of the polymerized matrix. $2x10^4$ green labeled VSMCs (PKH67 vital dye) were then added to ECs. Details are reported in Supplemental Materials.

Scratch assay on VSMCs. Scratch assays were performed on HG-cultured VSMCs, treated as indicated, to evaluate cell migration activity. VSMCs were seeded to a final density of 100,000 cells per well for 24h in order to allow cell adhesion and the formation of a confluent monolayer to occur. Details are reported in Supplemental Materials.

ELISA Assays. PDGF-BB concentration in D-CD31EVs were measured using a commercially available competitive enzyme immunoassay (ELISA) kit (R&D Systems, MN, USA), according to manufacturer's instructions. To evaluate mbPDGF-BB, intact or lysates D-CD31EVs ($2.5x10^8$ particles) were compared. The same samples were pre-treated with trypsin (0.25%) for 1h (negative control). Details are reported in Supplemental Materials.

Statistical analysis. All data are presented as mean ± SEM, unless otherwise reported. The D'Agostino–Pearson test was used to test normality. Data on *in vitro* angiogenesis, cell proliferation, ELISA, apoptosis and scratch assays, on qRT-PCR-miR expression, loss- and gain-of-function experiments, characterization of recovered EVs and, lastly, on the densitometric analysis for Western blots were analyzed using the Student *t* tests for 2-group comparison and using 1-way ANOVA, followed by Tukey's multiple comparison test, for ≥ 3 groups. All western blot experiments were performed in triplicate. The minimum sample size was four experiments performed in triplicate, thus ensuring 90% statistical power among experimental groups, and a probability level of 0.05, two-tailed hypothesis. The cut-off for statistical significance was set at $P < 0.05$. All statistical analyses were carried out using GraphPad Prism version 5.04 (Graph Pad Software, Inc).

RESULTS

D-CD31EVs potentiate VSMCs resistance to apoptosis in high glucose (HG) conditions

Circulating EVs are able to modulate cell fate (9,10,13). It was therefore decided to investigate whether and how circulating EVs, derived from ECs of T2D-individuals (D-EVs), may impact on VSMC fate. Guava analysis was used to demonstrate the presence of a high percentage of EVs of endothelial origin in the sera of non-diabetic (ND-EVs) and T2D individuals (Figure 1A). A significant reduction of EVs from T2D individuals was detected (Figure 1A). EC-derived EVs from sera were therefore isolated using CD31-coated magnetic beads (ND-CD31EVs and D-CD31EVs) and analyzed using transmission electron microscopy (Figure 1B) and western blot (Figure 1C). Functional studies were then performed to evaluate the biological relevance of D-CD31EVs in mediating VSMC dysfunction in hyperglycaemic condition (HG-culture condition). LG-conditioned VSMCs served as control. Consistent with data provided by Ruiz et al. (8), we found that, unlike LG, HG treatment was associated with a significant up-regulation of bcl-2 and down-regulation of bak/bax (Supplemental Figure S1A). By contrast the expression of another member of the bcl-2 protein family, bcl2l2, did not change (Supplemental Figure S1B). Moreover, HG treatment *per se* significantly decreased the number of apoptotic cells, without affecting VSMC proliferation (Supplemental Figure S1C-S1D). Functional studies were then performed on VSMCs cultured in HG conditions and treated with CD31EVs. As shown in Figure 1D, D-CD31EVs, unlike ND-CD31EVs, were able to further reduce both the number of apoptotic VSMCs and bak/bax content and increase bcl-2 level (Figure 1E).

D-CD31EVs are enriched in PDGF-BB

The transfer of proteins and/or genetic information into recipient cells is the main mechanism of EV action (9,10,13,14). CD31EV protein cargo and, in particular, the content of well-known VSMC proliferation/survival factor, PDGF-BB, were therefore analyzed in both CD31EVs and EVs

recovered from LG- and HG-treated ECs. Supplemental Figure S2A shows Nanosight analysis of EVs recovered from LG- or HG-cultured ECs (LG-EVs or HG-EVs). No differences in EV size and number between LG-EVs and HG-EVs were detected (data not shown). Conversely, PDGF-BB was found to be enriched only in D-CD31EVs (Figure 2A) and in HG-EVs (Supplemental Figure S2B).

Membrane bound-PDGF-BB drives D-CD31EV anti-apoptotic cues

LG- and HG-cultured VSMCs were treated with PDGF-BB in order to investigate the contribution of PDGF-BB in mediating D-CD31EV biological effects. In fact, PDGF-BB further increased bcl-2 content, while reducing the number of apoptotic cells and bak/bax content in HG-conditioned VSMCs. Conversely, these effects were not detected in VSMCs cultured in LG conditions (Figure 2B-2C). siRNA technology was therefore harnessed to abrogate PDGF-BB expression in EVs (Figure 2D-2E) and validate the role of PDGF-BB in regulating D-CD31EV survival signals in HG conditions. As expected, PDGF-BB-depleted EVs were no longer able to either increase bcl-2, or decrease bak/bax expression (Figure 2F) and the number of apoptotic cells (Figure 2G). To investigate whether different mechanisms might account for free PDGF-BB and D-CD31EV-PDGF-BB-induced effects, HG-cultured VSMCs were pre-treated with a blocking PDGFRβ antibody, stimulated with D-CD31EVs or free PDGF-BB, and analyzed for bak/bax and bcl-2 expression. As shown in Figure 3A PDGFRβ blockade impacts on both free PDGF-BB and D-CD31EVs-mediated bak/bax and bcl-2 expression. To rule out the possibility that this effect depended on inhibition of PDGFRβ-mediated EV internalization, Z-stack analysis was performed. Figure 3B shows that PDGFRβ blockade did not hamper EV internalization. Of note, the ELISA assay led to the discovery that PDGF-BB was anchored to the membrane of D-CD31EVs (Figure 3C) indicating that EV-mbPDGF-BB, by binding to the PDGFRβ, might drive D-CD31EV biological effects.

D-CD31EVs induce VSMC migration and recruitment to neovessels via PDGF-BB-mediated effects

CD31EVs were also evaluated in an EC/VSMC co-culture assay. A reduced number of vessels was detected in HG-cultured ECs (data not shown) and D-CD31EVs were nevertheless able to promote VSMC recruitment to neo-formed tubule-like structures (Figure 4A-4B), unlike ND-CD31EVs. A scratch assay also highlighted increased VSMC motility upon D-CD31EV treatment (Figure 4C). As shown in Supplemental Figure S2C, these effects did not depend on differences in EV-VEGF content. Furthermore, the contribution of PDGF-BB to both processes was validated in experiments using PDGF-BB-depleted EVs; such EVs failed to induce either effects (Figure 4D-F).

T2D individual-derived VSMCs express high bcl-2 and low bak/bax content

To validate the above results VSMCs isolated from either T2D (D) or non-diabetic (ND) human atherosclerotic plaque specimens were analyzed for bak/bax and bcl-2 expression. As shown in Figure 5A, the majority of the recovered cells express VSMC marker. Moreover, as previously reported by Ruiz et al. (8), it was confirmed that D-VSMCs expressed high bcl-2 levels. In addition, we found that D-VSMCs also expressed low bak/bax content (Figure 5B-5C).

miR-296-5p-post-transcriptionally controls bak level in response to HG and D-CD31EVs

To gain further insight into the mechanisms regulating VSMC fate the expression of miRs potentially involved in this process was first analyzed in D-VSMCs and compared to ND-VSMCs. As shown in Figure 6A, no significant differences were detected in the expression of miR-21-5p, miR-24-3p, miR-145, miR-29a (not included in the panel: CT>38), miR-221 and miR-222 between D- and ND-VSMCs (29-30). Moreover, since bak, unlike bax, is one of miR-296-5p putative target genes (TarBase v7.0) (31) its expression was also analyzed. Indeed, high miR-296-5p levels was detected in D-VSMCs (Figure 6A). In order to validate the role of miR-296-5p in controlling bak expression, VSMCs cultured in LG- or HG-conditions were analyzed for miR-296-5p expression. As shown in Figure 6B an increased miR-296-5p expression was detected upon HG treatment. Moreover, the depletion of miR-296-5p in HG-cultured VSMCs (Supplemental Figure S3) led to the decrease of

242 bcl-2 levels, the increase of bak/bax content (Figure 6C) and a consistent increase in the number of
243 apoptotic cells (Figure 6D). To confirm the role of miR-296-5p in bak post-transcriptional regulation,
244 the full-length 3′UTR *BAK1* nucleotide sequence was analyzed for miR-296-5p blasting sequences
245 revealing several base pairings (1138–1158bp) (Figure 7A). The luciferase assay was used to
246 demonstrate that bak is indeed a direct miR-296-5p target (Figure 7B). This observation was further
247 validated by gain-of-function experiments (Figure 7C-7D).

248 In order to investigate the contribution of PDGF-BB in mediating miR-296-5p expression, LG- and
249 HG-cultured VSMCs were also treated with PDGF-BB. As shown in Figure 6E, PDGF-BB further
250 increased miR-296-5p only in HG-cultured VSMCs. These results were validated by siRNA
251 technology (Figure 6F), thus suggesting that VSMC survival may be under the control of miR-296-
252 5p.

253 **D-CD31EVs are almost depleted of miR-296-5p content**

254 To exclude the possibility that D-CD31EV-mediated effects could also depend on the delivery of
255 miR-296-5p, the miR-296-5p content was also evaluated in CD31EVs and LG- or HG-cultured EC-
256 derived EVs (LG-EVs or HG-EVs). Almost undetectable levels of miR-296-5p were found in D-
257 CD31EVs (Supplemental Figure S2D) and in EVs from HG-treated ECs (Supplemental Figure S2E).
258 Thus, the role of mbPDGF-BB-D-CD31EVs in mediating miR-296-5p-driven post-transcriptional
259 regulation of bak and its down-stream events was further strengthened.

260

DISCUSSION

Atherosclerosis and its associated complications is a major cause of death worldwide (32). Diabetes accelerates atherosclerosis and restenosis after angioplasty (33,34). Indeed, increased VSMC migration and survival/proliferation are crucial for restenosis, particularly in diabetics (35-37). *In vitro* and *ex-vivo* studies have shown that the up-regulation of bcl-2/bcl-xl is crucial for VSMC resistance to apoptosis in diabetes (7,8,38,39). Moreover, Li H *et al.* (7) have reported that, while HG enhances the expression of bcl-2 family members in VSMCs, it reduced the expression of the IAP1. We herein demonstrate that VSMCs, exposed to HG concentrations, up-regulate bcl-2 and down-regulate bak/bax, without affecting VSMC proliferation. Moreover, we discovered that these effects are boosted by D-CD31EV treatment. A cell's survival or death depends on the integrity of the mitochondrial outer membrane (MOM) (40). In this regard, while the pro-apoptotic proteins, bak and bax, are involved in the permealization of MOM, the anti-apoptotic bcl-2 family members counteract such pro-apoptotic signals by preventing cytochrome *c* efflux (40). Our results therefore indicate that an additional shift in the balance, from apoptotic to anti-apoptotic signals, might be the main mechanism behind – D-CD31EVs-induced resistance to apoptosis in HG conditions, and suggest that hyperglycaemia-mediated cues preferentially translate into VSMC resistance towards apoptosis rather than VSMC proliferation.

The genetic material in EV cargo has sparked considerable interest. The role of miRs as mediators of epigenetic changes has been extensively reported, particularly in diabetes (41,42). The transfer of miRs into recipient cells has been described as a relevant mechanism of EV biological action (9-14). As a matter of fact, Gu et al. (43) recently reported that the transfer of miR-195 from EC-derived EVs to VSMCs regulates VSMC proliferation. Despite the ability of D-CD31EVs to induce functional changes in VSMCs, our results demonstrate that D-CD31EV-mediated VSMC dysfunction relies on a mechanism independent of the delivery of miRs. Indeed, EVs also transport and deliver proteins which can affect VSMC fate, including PDGF-BB. PDGF-BB is a growth factor

known to regulate VSMC outcomes (44,45). In this regard, PDGF-BB derived from platelet and EC is considered a relevant mediator of VSMC dysfunction and restenosis (46). As a matter of fact, we demonstrate that D-CD31EVs are enriched in PDGF-BB and that PDGF-BB enriched D-CD31EVs ~~may~~ contributes to VSMC dysfunction in diabetic setting. Several lines of evidence indicate that downstream signaling events, activated by PDGF-BB, trigger various biological processes, including VSMC migration and recruitment to neo-formed vessels (44,45). It is worth noting that PDGF-BB depleted EVs failed to induce both VSMC migration and recruitment to neovessels. This suggests that CD31EV-PDGF-BB cargo might play a crucial role in accelerating VSMC dysfunction and restenosis in T2D.

PDGF-BB synthesis and release can increase in response to various stimuli including intima damage (47). As shown herein, in diabetic setting, CD31EVs are a relevant circulating PDGF-BB reservoir and contribute to VSMC fate. We established that PDGF-BB is bound to the membrane of CD31EVs, and is required for their biological action but not for their internalization. As a proof of concept, PDGFRβ blockade completely hampers CD31EV-mediated bak/bax expression, without impeding their entry into the cell. This indicates that, along with free PDGF-BB, mbPDGF-BB enriched D-CD31EVs contribute to PDGF-BB paracrine effects (48). A co-operative action between CD31EVs and platelets-derived EVs could be postulated *in vivo.* In fact, EVs released from platelets accumulate in human atherosclerotic plaques and can induce major biological pathways by transferring their PDGF-BB content (49). In line with the results presented herein, it has been recently reported that EC- and platelet-derived EVs are enriched in PDGF-BB in patients with cardiovascular diseases (50).

miRs are key regulators of gene expression, mainly at the post-transcriptional level (51). We herein demonstrate, both *ex vivo* and *in vitro*, that the hyperglycaemia milieu enhances miR-296-5p expression and modulates bak content in VSMCs, and that these effects are strictly dependent on D-CD31EV-PDGF-BB cargo, rather than EV-miR-296-5p delivery. In addition, a shift between anti-apoptotic to pro-apoptotic signals after PDGFRβ blockade (down-regulation of bcl-2 expression) was

observed. This suggests that PDGF-BB directly, or indirectly by changing the balance of cellular miRs, might transcriptionally or post-transcriptionally regulate its expression. Mutually, these events translate in VSMC resistance to apoptosis.

Emerging evidence suggests that EVs can serve as specific diagnostic/prognostic biomarkers since they can provide intercellular state information on a given disease condition (52). Increased levels of "small (submicroscopic) membranous particles" of endothelial origin, such as $CD31^{+}$/annexin V^{+} and $CD31^{+}/CD42^{-}$, have been detected in circulation in patients with coronary artery disease (CAD), suggesting that they may be an additional risk stratification factor (18,19). A significant reduction in CD31EVs ($CD31^{high}/CD42b^{low}/CD14^{low}$) has been found in T2D individuals in the present study. The phenotype of the "small membrane particles", which also includes apoptotic bodies, and the lack of exosome refining (18,19) in CAD patient studies could explain the discrepancy with our results. However, increasing amounts of evidence indicate that healthy subjects and diseased individuals release EVs with different cargo.

Our *ex vivo* and *in vitro* results, reinforce the notion that D-CD31EV cargo, rather than D-CD31EV number, is the crucial determinant of their biological activity.

The present study reports that hyperglycaemia *per se* induces epigenetic mechanisms in VSMCs by enriching the circulating CD31EV cargo with mbPDGF-BB which translates into VSMC resistance to apoptosis (Figure 8). We are also the first to demonstrate that EV-mbPDGF-BB-mediated miR-296-5p overexpression and the post-transcriptional regulation of bak is a relevant mechanism of D-CD31EV action. Overall, these results identify D-CD31EV-mbPDGF-BB as a novel driver of VSMC dysfunction in diabetic setting.

ACKNOWLEDGEMENTS: Dr. MF Brizzi is the guarantor of this work, had full access to all data and takes full responsibility for data integrity and the accuracy of data analysis.

FUNDING: This work was supported by grants obtained by grant from the Ministero dell'Università e della Ricerca Scientifica (MIUR) ex 60% to PD, and by grant No. 071215 from Unicyte to GC and MFB. Associazione Italiana per la Ricerca sul Cancro (AIRC) project IG 2015.17630 to MFB.

DUALITY OF INTEREST

The authors declare that there is no duality of interest associated with this manuscript.

AUTHOR CONTRIBUTIONS

GT: performed *ex vivo* and *in vitro* experiments, EC-EV-miRs and protein analysis; PD: performed in vitro angiogenesis assay and FACS analysis; GL: performed in vitro experiments and EV isolation; AR: generated constructs and performed transfections; MG: performed loss- and gain-of-function approaches; SG: performed Western blot analysis; CG: performed EV isolation and characterization; AS: contributed to data interpretation and revised the manuscript; GC: contributed to the study conception and revised the manuscript; MFB: performed the study conception design and wrote the manuscript.

REFERENCES

1. Emerging Risk Factors Collaboration. Diabetes mellitus, fasting blood glucose concentration, and risk of vascular disease: a collaborative meta-analysis of 102 prospective studies. Lancet 2010;375:2215–2222
2. Fox CS, Golden SH, Anderson C, Bray GA, Burke LE, de Boer IH Bray GA, Burke LE, de Boer IH, Deedwania P, Eckel RH, Ershow AG, Fradkin J, Inzucchi SE, Kosiborod M, Nelson RG, Patel MJ, Pignone M, Quinn L, Schauer PR, Selvin E, Vafiadis DK; American Heart Association Diabetes Committee of the Council on Lifestyle and Cardiometabolic Health, Council on Clinical Cardiology, Council on Cardiovascular and Stroke Nursing, Council on Cardiovascular Surgery and Anesthesia, Council on Quality of Care and Outcomes Research, and the American Diabetes Association. Update on prevention of cardiovascular disease in adults with type 2 diabetes mellitus in light of recent evidence: a scientific statement from the American Heart Association and the American Diabetes Association. Circulation 2015;132:691–718
3. Terry JG, Tang R, Espeland MA, Davis DH, Vieira JL, Mercuri MF, Crouse JR 3rd. Carotid arterial structure in patients with documented coronary artery disease and disease-free control subjects. Circulation 2003;107:1146-1151
4. Schram MT, Henry RM, van Dijk RA, Kostense PJ, Dekker JM, Nijpels G, Heine RJ, Bouter LM, Westerhof N, Stehouwer CD. Increased central artery stiffness in impaired glucose metabolism and type 2 diabetes: the Hoorn Study. Hypertension 2004;43:176-81
5. Gomez D, Owens GK. Smooth muscle cell phenotypic switching in atherosclerosis. Cardiovasc Res 2012;95:156–164
6. Goel SA, Guo LW, Liu B, Kent KC. Mechanisms of post-intervention arterial remodelling. Cardiovasc Res 2012;96:363-371
7. Li H, Télémaque S, Miller RE, Marsh JD. High glucose inhibits apoptosis induced by serum deprivation in vascular smooth muscle cells via upregulation of Bcl-2 and Bcl-xl. Diabetes 2005;54:540-545
8. Ruiz E, Gordillo-Moscoso A, Padilla E, Redondo S, Rodriguez E, Reguillo F, Briones AM, van Breemen C, Okon E, Tejerina T. Human vascular smooth muscle cells from diabetic patients are resistant to induced apoptosis due to high Bcl-2 expression. Diabetes 2006;55:1243-1251
9. Simons M, Raposo G. Exosomes—vesicular carriers for intercellular communication. Curr Opin Cell Biol 2009;21:575–581
10. Mause SF, Weber C. Microparticles: protagonists of a novel communication network for intercellular information exchange. Circ Res 2010;107:1047–1057
11. Théry C, Ostrowski M, Segura E. Membrane vesicles as conveyors of immune responses. Nat Rev Immunol 2009;9:581-593
12. Gould SJ, Raposo G. As we wait: coping with an imperfect nomenclature for extracellular vesicles. J Extracell Vesicles 2013;2
13. Camussi G, Deregibus MC, Bruno S, Cantaluppi V, Biancone L. Exosomes/microvesicles as a mechanism of cell-to-cell communication. Kidney Int 2010;78:838-848
14. Ratajczak MZ, Ratajczak J. Horizontal transfer of RNA and proteins between cells by extracellular microvesicles: 14 years later. Clin Transl Med 2016;5:7
15. Yuana Y, Sturk A, Nieuwland R. Extracellular vesicles in physiological and pathological conditions. Blood Rev 2013;27:31-39

16. Chironi G, Simon A, Hugel B, Del Pino M, Gariepy J, Freyssinet JM, Tedgui A. Circulating leukocyte-derived microparticles predict subclinical atherosclerosis burden in asymptomatic subjects. Arterioscler Thromb Vasc Biol 2006;26:2775-2780
17. Ueba T, Nomura S, Inami N, Nishikawa T, Kajiwara M, Iwata R, Yamashita K. Plasma level of platelet-derived microparticles is associated with coronary heart disease risk score in healthy men. J Atheroscler Thromb 2010;17:342-349
18. Sinning JM, Losch J, Walenta K, Böhm M, Nickenig G, Werner N. Circulating CD31+/Annexin V+ microparticles correlate with cardiovascular outcomes. Eur Heart J 2011;32:2034-2041
19. Jung KH, Chu K, Lee ST. Bahn JJ, Kim JH, Kim M, Lee SK, Roh JK. Risk of macrovascular complications in type 2 diabetes mellitus: endothelial microparticle profiles. Cerebrovasc Dis 2011;31:485-493
20. Brizzi MF, Formato L, Dentelli P, Rosso A, Pavan M, Garbarino G, Pegoraro M, Camussi G, Pegoraro L. Interleukin-3 stimulates migration and proliferation of vascular smooth muscle cells: a potential role in atherogenesis. Circulation 2001;103:549-554
21. Togliatto G, Dentelli P, Gili M, Gallo S, Deregibus C, Biglieri E, Iavello A, Santini E, Rossi C, Solini A, Camussi G, Brizzi MF. Obesity reduces the pro-angiogenic potential of adipose tissue stem cell-derived extracellular vesicles (EVs) by impairing miR-126 content: impact on clinical applications. Int J Obes (Lond) 2016;40:102-111
22. Deregibus MC, Cantaluppi V, Calogero R, Lo Iacono M, Tetta C, Biancone L, Bruno S, Bussolati B, Camussi G. Endothelial progenitor cell derived microvesicles activate an angiogenic program in endothelial cells by a horizontal transfer of mRNA. Blood 2007;110:2440-2448
23. Bruno S, Grange C, Collino F, Deregibus MC, Cantaluppi V, Biancone L, Tetta C, Camussi G. Microvesicles derived from mesenchymal stem cells enhance survival in a lethal model of acute kidney injury. PLoS One 2012;7:e33115
24. Greening DW, Xu R, Ji H, Tauro BJ, Simpson RJ. A protocol for exosome isolation and characterization: evaluation of ultracentrifugation, density-gradient separation, and immunoaffinity capture methods. Methods Mol Biol 2015;1295:179-209
25. Lombardo G, Dentelli P, Togliatto G, Rosso A, Gili M, Gallo S, Deregibus MC, Camussi G, Brizzi MF. Activated stat5 trafficking via endothelial cell-derived extracellular vesicles controls IL-3 pro-angiogenic paracrine action. Sci Rep 2016;6:25689
26. Gallo S, Gili M, Lombardo G, Rossetti A, Rosso A, Dentelli P, Togliatto G, Deregibus MC, Taverna D, Camussi G, Brizzi MF. Stem Cell-Derived, microRNA-Carrying Extracellular Vesicles: A Novel Approach to Interfering with Mesangial Cell Collagen Production in a Hyperglycaemic Setting. PLoS One 2016;11:e0162417
27. Dentelli P, Barale C, Togliatto G, Trombetta A, Olgasi C, Gili M, Riganti C, Toppino M, Brizzi MF. A diabetic milieu promotes OCT4 and NANOG production in human visceral-derived adipose stem cells. Diabetologia 2013;56:173-184
28. Zeoli A, Dentelli P, Rosso A, Togliatto G, Trombetta A, Damiano L, di Celle PF, Pegoraro L, Altruda F, Brizzi MF. Interleukin-3 promotes expansion of hemopoietic-derived CD45+ angiogenic cells and their arterial commitment via STAT5 activation. Blood 2008;112:350-361
29. Shantikumar S, Caporali A, Emanueli C. Role of microRNAs in diabetes and its cardiovascular complications. Cardiovasc Res 2012;93:583-593

30. Wei Y, Schober A, Weber C. Pathogenic arterial remodeling: the good and bad of microRNAs. Am J Physiol Heart Circ Physiol. 2013;304:H1050-1059.
31. Karginov FV, Hannon GJ Remodeling of Ago2-mRNA interactions upon cellular stress reflects miRNA complementarity and correlates with altered translation rates. Genes Dev 2013;27:1624-1632
32. GBD 2013 Mortality and Causes of Death Collaborators. Global, regional, and national age-sex specific all-cause and cause-specific mortality for 240 causes of death, 1990-2013: a systematic analysis for the Global Burden of Disease Study 2013. Lancet 2015;385:117-171
33. Kornowski R, Mintz GS, Kent KM, Pichard AD, Satler LF, Bucher TA, Hong MK, Popma JJ, Leon MB. Increased restenosis in diabetes mellitus after coronary interventions is due to exaggerated intimal hyperplasia. A serial intravascular ultrasound study. Circulation 1997;95:1366-1369
34. Brooks MM, Jones RH, Bach RG. Chaitman BR, Kern MJ, Orszulak TA, Follmann D, Sopko G, Blackstone EH, Califf RM. Predictors of mortality and mortality from cardiac causes in the bypass angioplasty revascularization investigation (BARI) randomized trial and registry. For the BARI Investigators. Circulation 2000;101:2682-2689
35. Henry RM, Kostense PJ, Dekker JM, Nijpels G, Heine RJ, Kamp O, Bouter LM, Stehouwer CD. Carotid arterial remodeling: a maladaptive phenomenon in type 2 diabetes but not in impaired glucose metabolism: the Hoorn study. Stroke 2004;35:671-676
36. Watson PA, Nesterova A, Burant CF, Klemm DJ, Reusch JE. Diabetes-related changes in cAMP response element-binding protein content enhance smooth muscle cell proliferation and migration. J Biol Chem 2001;276:46142-46150
37. Yasunari K, Kohno M, Kano H, Yokokawa K, Minami M, Yoshikawa J. Antioxidants improve impaired insulin-mediated glucose uptake and prevent migration and proliferation of cultured rabbit coronary smooth muscle cells induced by high glucose. Circulation 1999;99:1370-1378
38. Hall JL, Matter CM, Wang X, Gibbons GH. Hyperglycemia inhibits vascular smooth muscle cell apoptosis through a protein kinase C-dependent pathway. Circ Res 2000;87:574-580
39. Sakuma H, Yamamoto M, Okumura M, Kojima T, Maruyama T, Yasuda K. High glucose inhibits apoptosis in human coronary artery smooth muscle cells by increasing bcl-xL and bfl-1/A1. Am J Physiol Cell Physiol 2002;283:C422-C428
40. Karch J, Molkentin JD. Regulated necrotic cell death: the passive aggressive side of Bax and Bak. Circ Res 2015;116:1800-1809
41. Guay C, Regazzi R. Circulating microRNAs as novel biomarkers for diabetes mellitus. Nat Rev Endocrinol 2013;9:513-521
42. Togliatto G, Dentelli P, Brizzi MF. Skewed Epigenetics: An Alternative Therapeutic Option for Diabetes Complications. J Diabetes Res 2015;2015:373708
43. Gu J, Zhang H, Ji B, Jiang H, Zhao T, Jiang R, Zhang Z, Tan S, Ahmed A, Gu Y. Vesicle miR-195 derived from Endothelial Cells Inhibits Expression of Serotonin Transporter in Vessel Smooth Muscle Cells. Sci Rep. 2017;7:43546
44. Grotendorst CR, Chang T, Seppa HEJ, Kleinman HK, Martin GR. Platelet-derived growth factor is a chemoattractant for vascular smooth muscle cells. J Cell Physiol 1982;113:261–266

45. Bilato C, Pauly RR, Melillo G, Monticone R, Gorelick-Feldman D, Gluzband YA, Sollott SJ, Ziman B, Lakatta EG, Crow MT. Intracellular signaling pathways required for rat vascular smooth muscle cell migration. Interactions between basic fibroblast growth factor and platelet-derived growth factor. J Clin Invest 1995;96:1905-1915
46. McNamara CA, Sarembock IJ, Bachhuber BG, Stouffer GA, Ragosta M, Barry W, Gimple LW, Powers ER, Owens GK. Thrombin and vascular smooth muscle cell proliferation: implications for atherosclerosis and restenosis. Semin Thromb Hemost 1996;22:139-144
47. Andrae J, Gallini R, Betsholtz C. Role of platelet-derived growth factors in physiology and medicine. Genes Dev 2008;22:1276-1312
48. Raines EW. PDGF and cardiovascular disease. Cytokine Growth Factor Rev 2004;15:237-254
49. Weber A, Köppen HO, Schrör K. Platelet-derived microparticles stimulate coronary artery smooth muscle cell mitogenesis by a PDGF-independent mechanism. Thromb Res 2000;98:461–466
50. Goetzl EJ, Schwartz JB, Mustapic M, Lobach IV, Daneman R, Abner EL, Jicha GA. Altered cargo proteins of human plasma endothelial cell-derived exosomes in atherosclerotic cerebrovascular disease. FASEB J 2017;31:3689-3694
51. Tüfekci KU, Meuwissen RL, Genç S. The role of microRNAs in biological processes. Methods Mol Biol 2014;1107:15-31
52. Barile L, Vassalli G. Exosomes: Therapy delivery tools and biomarkers of diseases. Pharmacol Ther 2017;pii:S0163-7258(17)30034-7
53. Pant S, Hilton H, Burczynski ME. The multifaceted exosome: biogenesis, role in normal and aberrant cellular function, and frontiers for pharmacological and biomarker opportunities. Biochem Pharmacol 2012;83:1484-1494

511 **FIGURE LEGENDS**

512 **Figure 1. D-CD31EVs increase VSMC survival. (A)** Representative FACS analysis of EVs
513 recovered from sera of T2D (D, n=11) and ND individuals (ND, n=6); CD42b-FITC, CD14-PE and
514 CD31-APC were analyzed. All data are reported in the histograms (mean of percentage±SD) (*p<0.01*,
515 D-EVs vs ND-EVs for all markers). Isotype controls were included. **(B)** Representative transmission
516 electron microscopy (TEM) imaging of D- and ND-CD31EVs negatively stained with NanoVan.
517 JEOL Jem 1010 electron microscope was used (black bars= 100 nm). **(C)** CD31EVs were lysed and
518 evaluated for CD31 content (CD31+), normalized to CD63. CD31EV negative (CD31-) fraction was
519 used as the negative control. The results are representative of all samples (D, n=11; ND, n=6)
520 (*p<0.001*, CD31+ vs CD31- fraction of T2D and non-diabetic individuals). **(D)** Apoptosis assay was
521 applied to HG-cultured VSMCs, treated as indicated (percentage±SEM of total apoptotic cells, n=6).
522 Doxorubicin (1μmol/l) was used as positive control (c+) (*p<0.001*, all experimental conditions vs
523 control (c+); *p<0.001*, D-CD31EVs vs ND-CD31EVs and none). **(E)** Cell extracts from HG-cultured
524 VSMCs, treated with D-CD31EVs or ND-CD31EVs, were analyzed for bak/bax and bcl-2 content,
525 normalized to α-SMA (*p<0.001*, D-CD31EVs vs ND-CD31EVs and none for bak; *p<0.05*, D-
526 CD31EVs vs ND-CD31EVs and none for bax and bcl-2, n=6).

527 **Figure 2. D-CD31EVs enriched in PDGF-BB induce anti-apoptotic signals (A)**. Negative and
528 positive fractions of CD31EVs were analyzed by western blot for PDGF-BB, normalized to CD63.
529 The results are representative of all samples (D, n=11; ND, n=6) (*p<0.001*, CD31EVs+ vs CD31EVs-
530 of D and ND; *p<0.001*, D-CD31EVs+ vs ND-CD31EVs+ for PDGF-BB). **(B)** Cell extracts from LG-
531 and HG-cultured VSMCs untreated or treated with PDGF-BB (10 ng/ml), were analyzed for bak/bax
532 and bcl-2 content, normalized to α-SMA (PDGF-BB vs none in HG-cultured VSMCs*, p<0.001* for
533 bak and bax, *p=0.04* for bcl-2, n=5). **(C)** Apoptosis assay was applied to VSMCs, treated as above
534 (percentage±SEM of total apoptotic cells, n=6). Doxorubicin (1μmol/l) served as positive control
535 (c+) (LG-cultured VSMCs, *p=0.05*, all experimental conditions vs positive control (c+); HG-cultured

VSMCs, *p=0.001*, all experimental conditions vs positive control (c+), *p=0.008*, PDGF-BB vs none). **(D)** PDGF-BB content was evaluated in HG-cultured ECs transfected or not for 48h with siRNA empty vector, used as control (control siRNA), or with PDGF-BB siRNA, and normalized to β-actin (*p=0.007*, PDGF-BB siRNA vs none and *p=0.003*, PDGF-BB siRNA vs control siRNA). **(E)** PDGF-BB content was evaluated in EVs recovered from HG-cultured ECs, treated as above, and normalized to CD63 (*p<0.001*, PDGF-BB siRNA vs control siRNA and none). **(F)** Cell extracts from HG-cultured VSMCs, treated as indicated, were analyzed for bak/bax and bcl-2 content, normalized to α-SMA (*p<0.01*, HG-EVs PDGF-BB siRNA vs HG-EVs control and none; n=6). **(G)** Apoptosis assay was performed in HG-cultured VSMCs, treated as indicated (percentage±SEM of total apoptotic cells, n=6). Doxorubicin (1μmol/l) served as positive control (c+) (*p<0.001*, all experimental conditions vs positive control (c+); *p=0.02*, HG-EVs control siRNA vs none; *p=0.009,* HG-EVs PDGF-BB siRNA vs HG-EVs control siRNA).

Figure 3. PDGFRβ blockade interferes with free PDGF-BB- and D-CD31EV-mediated effects. **(A)** HG-cultured VSMCs, pre-incubated or not with a blocking PDGFRβ antibody (5μg/ml), were untreated or treated with PDGF-BB (10 ng/ml) or with D-CD31EVs for 24h. Cell extracts were analyzed for bak/bax and bcl-2 content, normalized to α-SMA (*p<0.001*, PDGF-BB and D-CD31EVs vs PDGF-BB and D-CD31EVs, pre-treated with anti-PDGFRβ antibody) (n=4). **(B)** VSMC-D-CD31EV up-take. VSMCs, pre-incubated or not with the blocking PDGFRβ antibody, were evaluated for the uptake of PKH26-labeled D-CD31EVs and analyzed. DAPI was used as nuclear marker. Representative sections (first-middle-last) of images (Z-stack) obtained on a confocal microscope are reported. Four different experiments performed in triplicate (n=4). Scale bars indicate 10 μm. **(C)** To evaluate mbPDGF-BB, intact or lysates D-CD31EVs ($2.5x10^8$ particles), untreated or treated with trypsin (0,25%) for 1h, were measured using a competitive enzyme immunoassay (ELISA) kit (** *p<0.01,* D-CD31EVs intact and lysates vs D-CD31EVs +trypsin) (n=3).

Figure 4. D-CD31EVs increase VSMC migration and recruitment to tubule-like structures. (A-B) An *in vitro* angiogenesis assay was performed using pre-labeled ECs (red) and VSMCs (green) co-cultured in HG medium with or without the indicated CD31EVs for 6h (scale bars=20μm, 40X magnification). Data are reported in the histogram as number±SEM of VSMCs per number of tubular structures (*p<0.001*, ND-CD31EVs vs none and D-CD31EVs; *p<0.05*, D-CD31EVs vs none, n=5). **(C)** VSMC migration assay was performed in HG conditions and the indicated treatment. (n=5, 20X magnification) (*p=0.04*, D-CD31EVs vs none; *p=0.01,* D-CD31EVs vs ND-CD31EVs). **(D-E)** An *in vitro* angiogenesis assay was performed, as above, using HG-EVs control siRNA or HG-EVs depleted of PDGF-BB (PDGF-BB siRNA) (scale bars=20μm, 40X magnification). Data are reported in the histogram as number±SEM of VSMCs per number of tubular structures (*p<0.001*, HG-EVs PDGF-BB siRNA vs HG-EVs control siRNA and none, n=5). **(F)** VSMC migration assay was performed in HG conditions under the indicated treatment (n=5, 20X magnification) (*p=0.009*, HG-EVs PDGF-BB siRNA vs HG-EVs control siRNA). Representative images were acquired on a confocal microscope.

Figure 5. VSMCs from T2D individuals express high levels of bcl-2 and low bak/bax content. (A) Representative FACS analysis of CD31 and alpha-smooth muscle cell (α-SMA) surface markers expressed by VSMCs recovered from T2D (D, n=11) and non-diabetic (ND) individuals (ND, n=6). All data are reported in the Table (mean percentage±SD). Isotype control was included. **(B)** bak/bax and bcl-2 content was analyzed on all ND- or D-VSMC samples, normalized to α-SMA content. The statistical analysis of all samples (D, n=11; ND, n=6) is reported in **(C)** (*p<0.01,* D vs ND for bak, *p<0.001,* D vs ND for bax*, p<0.05,* D vs ND for bcl-2).

Figure 6. VSMC miR-296-5p expression is increased in hyperglycaemic condition and boosted by PDGF-BB (A) The indicated miRs were evaluated by qRT-PCR in VSMCs recovered from T2D (D) and ND human atherosclerotic plaque specimens. Data normalized to RNU6B are representative of all samples (D, n=11; ND, n=6) (*p=0.02*, D vs ND for miR-296-5p). **(B)** miR-296-5p was evaluated

585 by qRT-PCR on LG- or HG-treated VSMCs and normalized to RNU6B (*p=0.03*, HG- vs LG-treated
586 VSMCs, n=6). **(C)** Loss-of-function experiments were performed on LG- and HG-cultured VSMCs
587 for 48h, using antago-miR control or antago-miR-296-5p oligonucleotides. After 48h cells were lysed
588 and analyzed for bak/bax and bcl-2 content, normalized to α-SMA (*p<0.001*, LG-antago-miR control
589 and LG-anti-miR-296-5p vs HG-antago-miR control for bak/bax and bcl-2; *p<0.001*, HG-antago-
590 miR control vs HG-antago-miR-296-5p for bak and bcl-2; *p<0.05*, HG-antago-miR control vs HG-
591 antago-miR-296-5p for bax, n=3). **(D)** Apoptosis assay was performed on VSMCs cultured and
592 treated as in (C). Doxorubicin (1μmol/l) served as positive control (c+). Data are expressed as
593 percentage±SEM (n=5) of total apoptotic cells (*p<0.001*, LG-antago-miR control vs HG- antago-miR
594 control, HG- antago-miR control vs HG-antago-miR-296-5p; *p<0.001*, all experimental conditions
595 vs control, c+). **(E)** miR-296-5p expression, normalized to RNU6B, was evaluated by qRT-PCR in
596 LG and HG-cultured VSMCs both with and without PDGF-BB (10 ng/ml) (*p=0.002*, PDGF-BB vs
597 none in HG-treated VSMCs, n=6). **(F)** miR-296-5p expression, normalized to RNU6B, was evaluated
598 by qRT-PCR in HG-cultured VSMCs, treated as indicated (*p=0.007*, HG-EVs control siRNA vs
599 none; *p=0.002*, HG-EVs PDGF-BB siRNA vs HG-EVs control siRNA, n=6).

600 **Figure 7. miR-296-5p post-transcriptionally regulates bak expression. (A)** Blast analysis of hsa-
601 miR-296-5p sequence and *BAK1* 3′UTR full-length shows a base pairing from 1138 to 1158 bp. **(B)**
602 pGL3 empty vector and pGL3-3′UTR *BAK1* luciferase constructs were transfected into LG- and HG-
603 cultured VSMCs. Relative luciferase activity is reported (*p<0.001* HG vs LG in pGL3–3′UTR *BAK1*-
604 transfected cells, n=5). **(C)** pGL3 and pGL3-3′UTR *BAK1* constructs were transfected into LG-
605 cultured VSMCs previously transfected with pre-miR control or with pre-miR-296-5p. Relative
606 luciferase activity is reported (*p<0.001* pre-miR-296-5p vs pre-miR control in pGL3–3′UTR *BAK1*
607 transfected cells, n=5). **(D)** Bak content was analyzed on cell extracts from VSMCs overexpressing
608 miR-296-5p (pre-miR-296-5p), not transfected or transfected with pGL3 or pGL3-3′UTR *BAK1*

609 constructs and normalized to α-SMA (*p<0.001* VSMCs/pre-miR-296-5p none and pGL3 vs
610 VSMCs/pre-miR-296-5p+pGL3-3′UTR *BAK1,* n=5).

611 **Figure 8. Schematic representation of HG and D-CD31EV mechanism of action.** ND-CD31EVs
612 do not affect VSMC fate due to their low mbPDGF-BB content (left panel). In the diabetic setting,
613 D-CD31EVs enriched in mbPDGF-BB content affect VSMC fate by promoting resistance to
614 apoptosis (right panel).

Figure 1

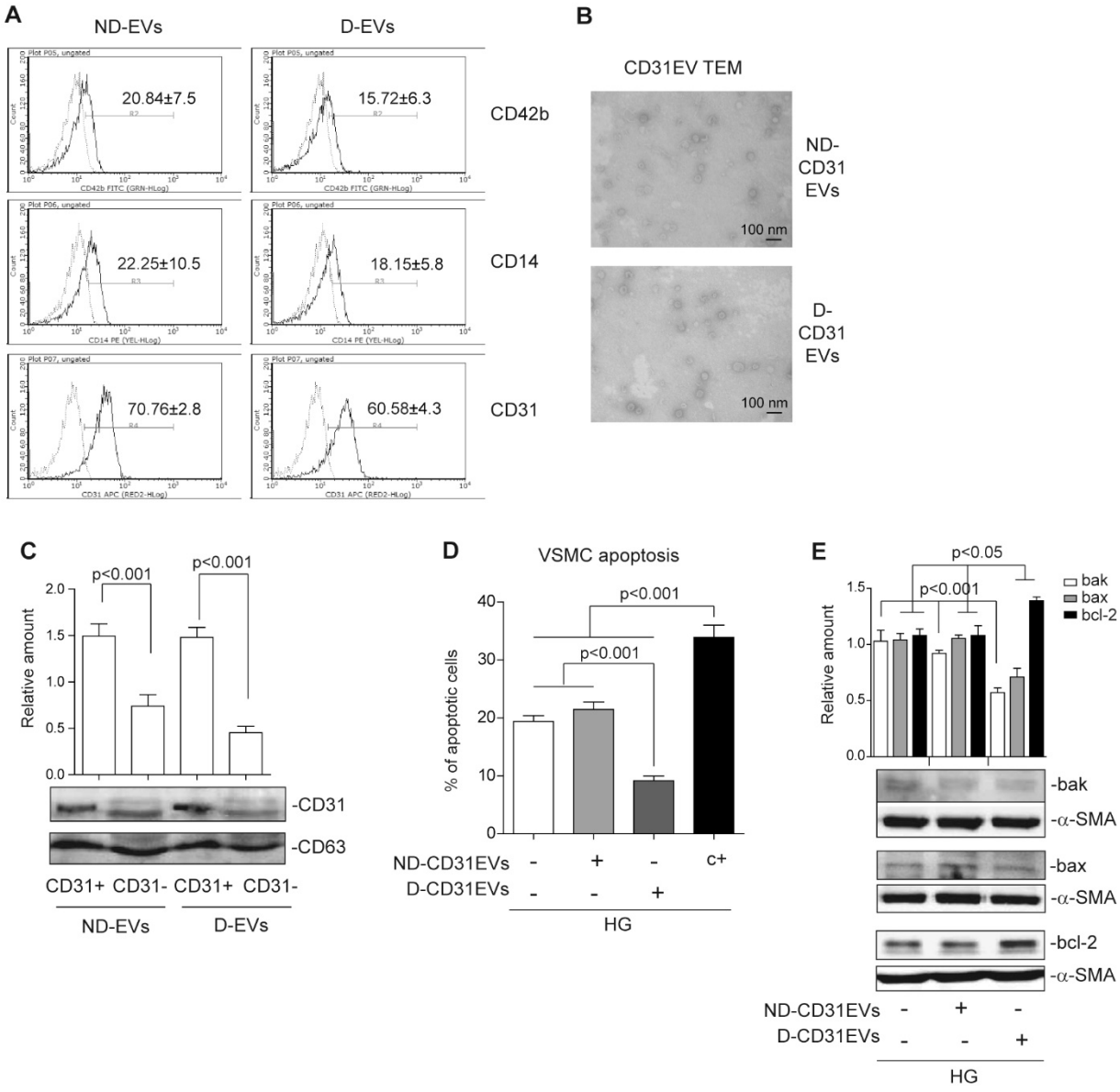

615

616

Figure 2

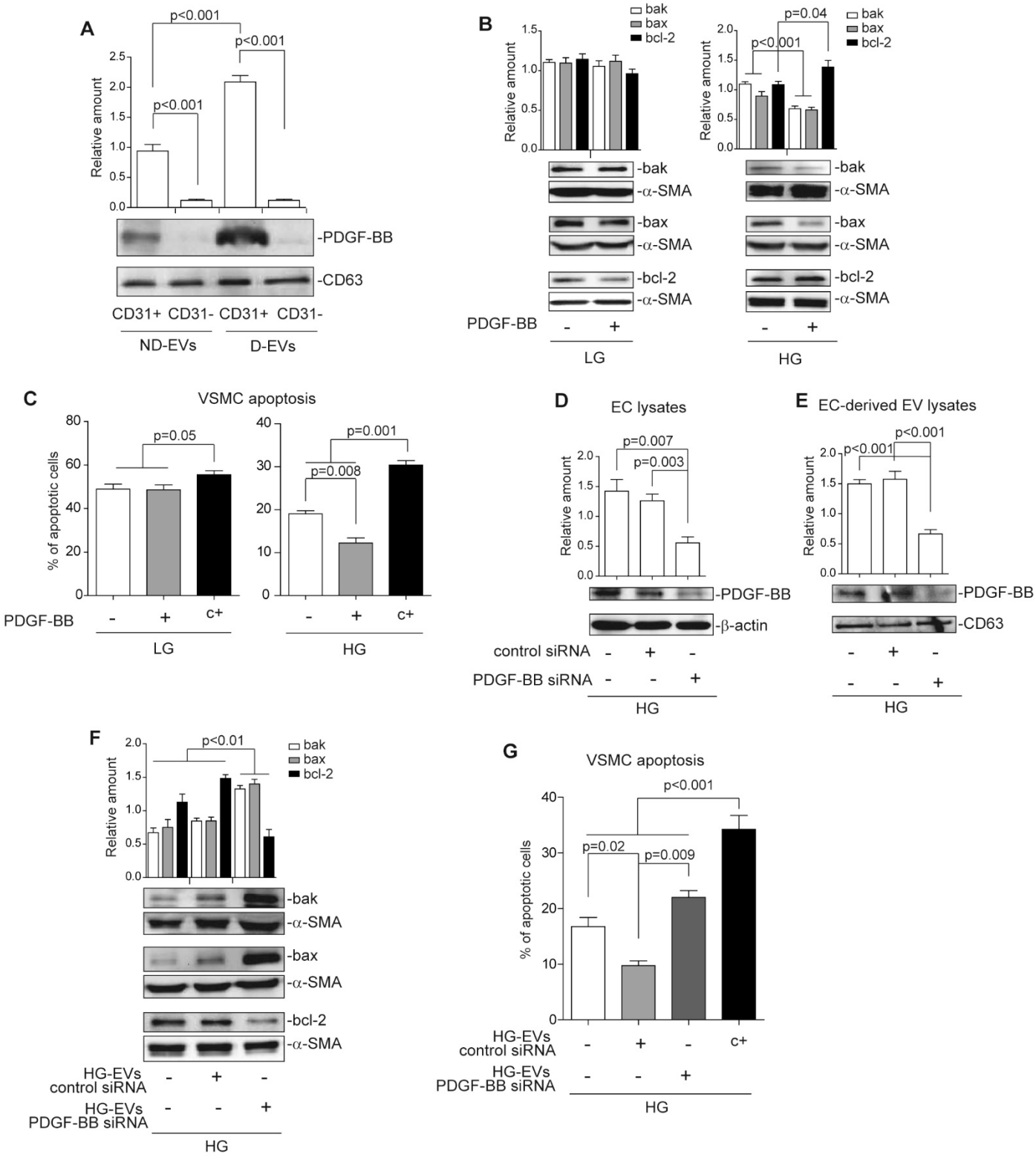
A
p<0.001
p<0.001
p<0.001
Relative amount
-PDGF-BB
-CD63
CD31+ CD31- CD31+ CD31-
ND-EVs
D-EVs
B
bak
bax
bcl-2
Relative amount
p=0.04
p<0.001
-bak
-α-SMA
-bax
-α-SMA
-bcl-2
-α-SMA
PDGF-BB
LG
HG
C
VSMC apoptosis
% of apoptotic cells
p=0.05
p=0.001
p=0.008
PDGF-BB
LG
HG
D
EC lysates
Relative amount
p=0.007
p=0.003
-PDGF-BB
-β-actin
control siRNA
PDGF-BB siRNA
HG
E
EC-derived EV lysates
Relative amount
p<0.001
p<0.001
-PDGF-BB
-CD63
HG
F
p<0.01
bak
bax
bcl-2
Relative amount
-bak
-α-SMA
-bax
-α-SMA
-bcl-2
-α-SMA
HG-EVs control siRNA
HG-EVs PDGF-BB siRNA
HG
G
VSMC apoptosis
% of apoptotic cells
p<0.001
p=0.02
p=0.009
HG-EVs control siRNA
HG-EVs PDGF-BB siRNA
HG

620

Figure 3

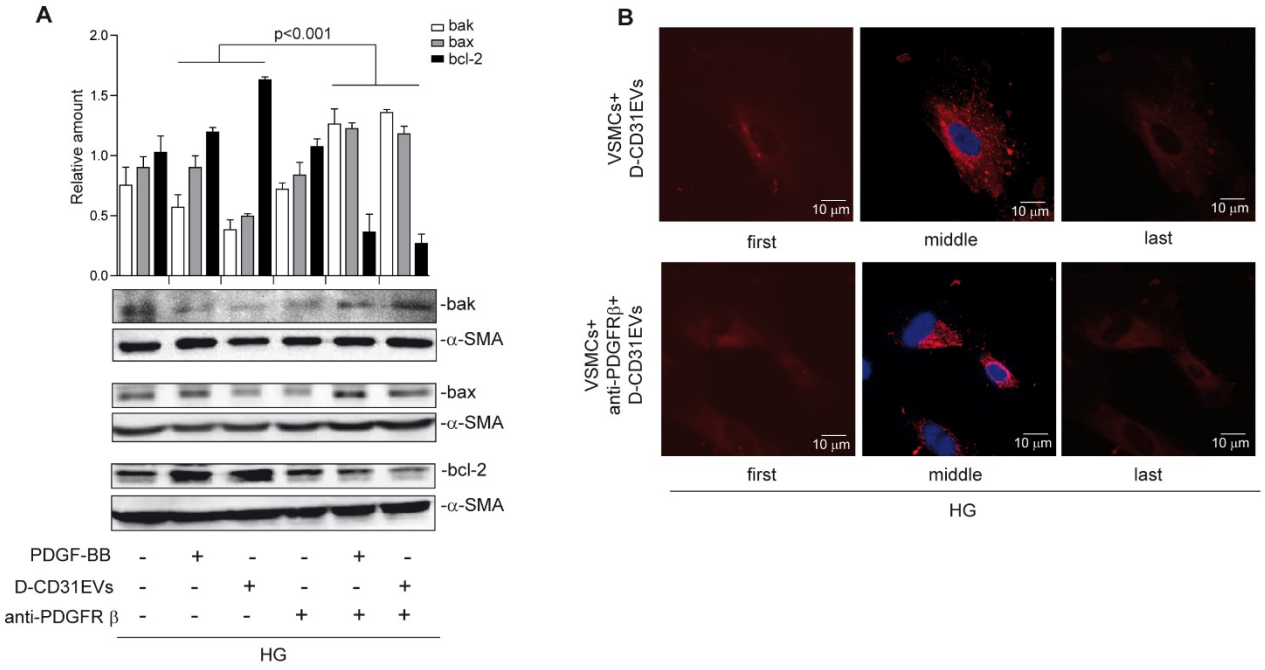

C

PDGF-BB (pg/ml)	
D-CD31EVs	25±4.7
D-CD31EV lysates	27±6.2
D-CD31EVs + trypsin	<15**

621

Figure 4

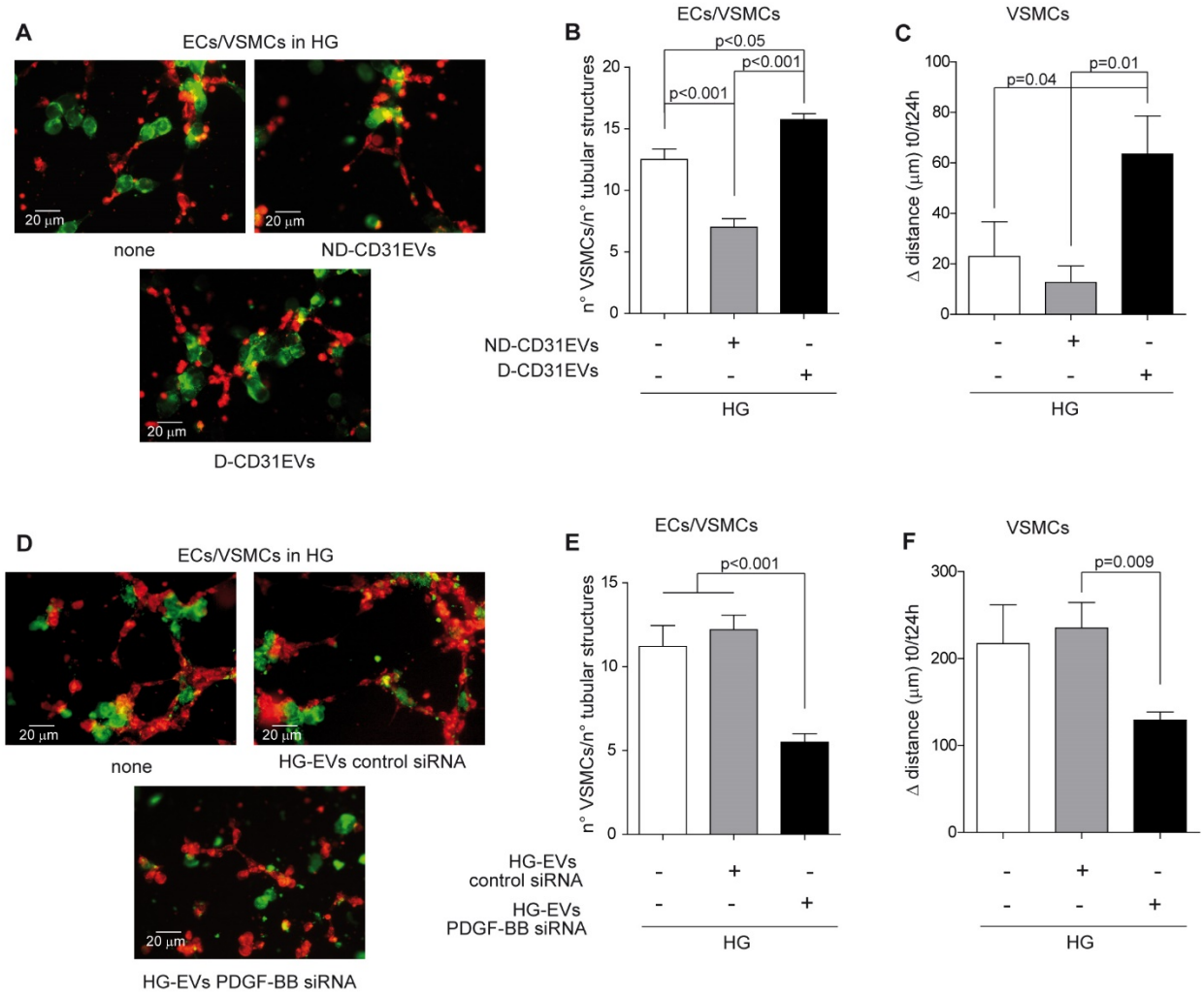
A
ECs/VSMCs in HG
20 µm
none
ND-CD31EVs
D-CD31EVs
B
ECs/VSMCs
p<0.05
p<0.001
p<0.001
n° VSMCs/n° tubular structures
ND-CD31EVs
D-CD31EVs
HG
C
VSMCs
p=0.04
p=0.01
Δ distance (µm) t0/t24h
HG
D
ECs/VSMCs in HG
none
HG-EVs control siRNA
HG-EVs PDGF-BB siRNA
E
ECs/VSMCs
p<0.001
n° VSMCs/n° tubular structures
HG-EVs control siRNA
HG-EVs PDGF-BB siRNA
HG
F
VSMCs
p=0.009
Δ distance (µm) t0/t24h
HG

622

Figure 5

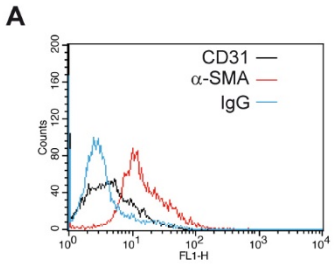

Marker	*ND*	*D*
CD31	22±4	26±5
α-SMA	72±9	76±10

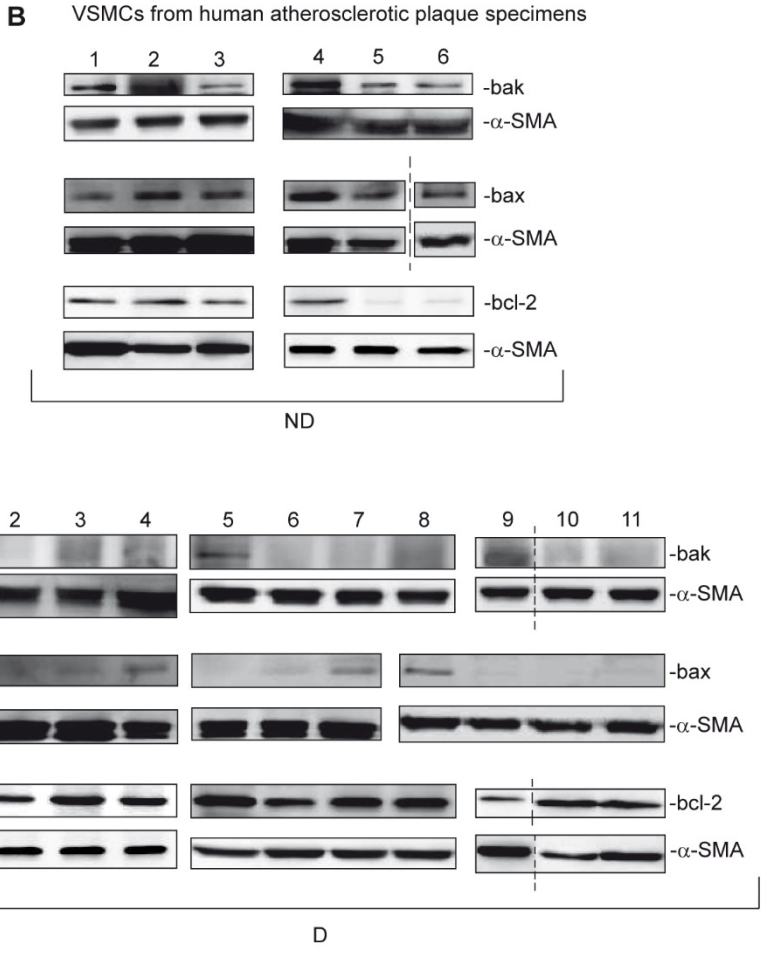

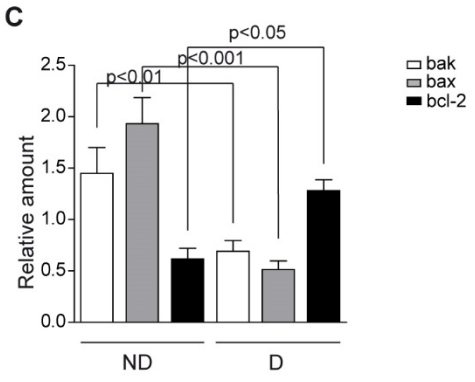

623

Figure 6

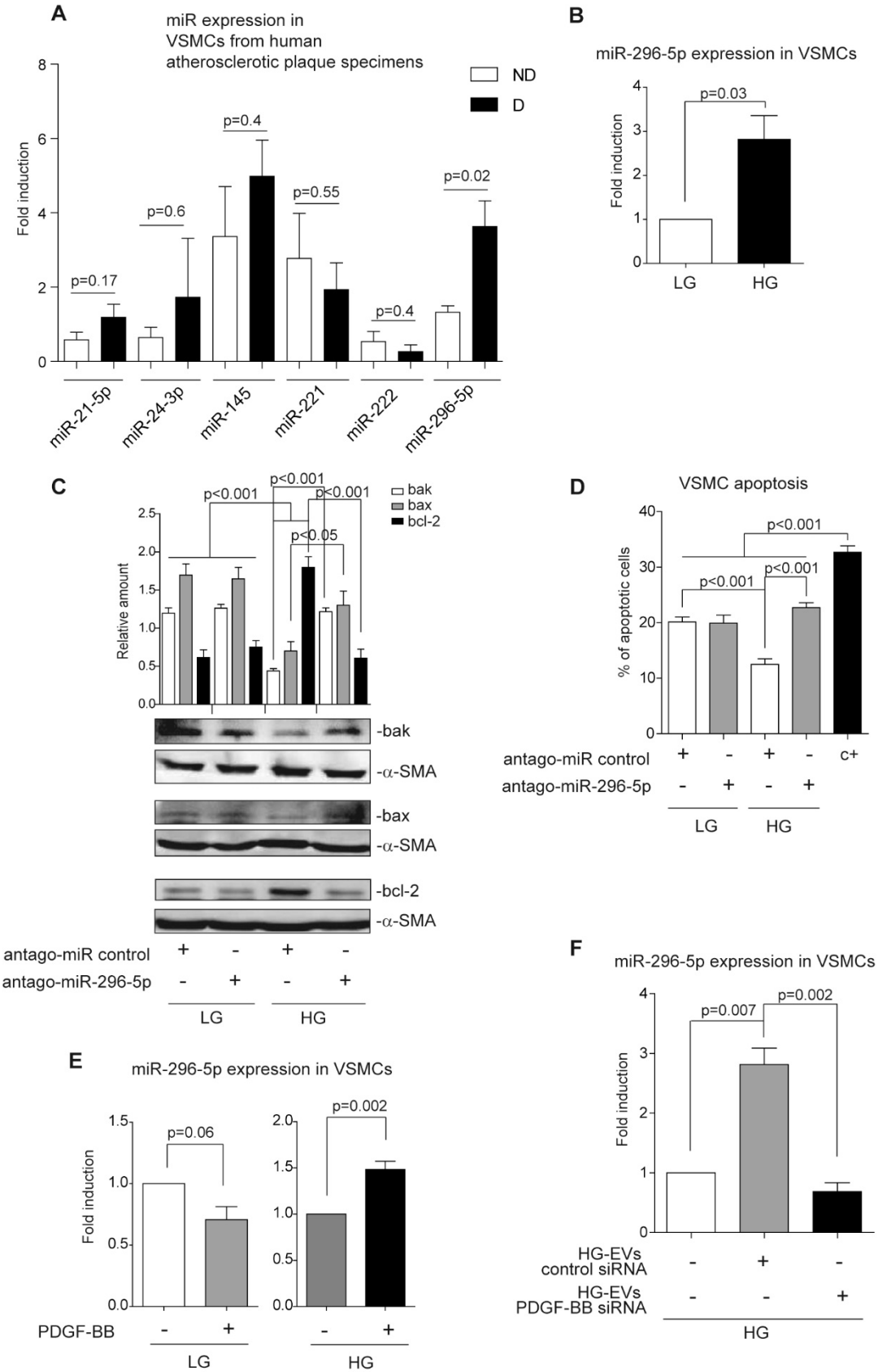
A
miR expression in VSMCs from human atherosclerotic plaque specimens
ND
D
Fold induction
p=0.17
p=0.6
p=0.4
p=0.55
p=0.4
p=0.02
miR-21-5p
miR-24-3p
miR-145
miR-221
miR-222
miR-296-5p
B
miR-296-5p expression in VSMCs
p=0.03
Fold induction
LG
HG
C
bak
bax
bcl-2
Relative amount
p<0.001
p<0.001
p<0.001
p<0.05
-bak
-α-SMA
-bax
-α-SMA
-bcl-2
-α-SMA
antago-miR control
antago-miR-296-5p
LG
HG
D
VSMC apoptosis
% of apoptotic cells
p<0.001
p<0.001
p<0.001
antago-miR control
antago-miR-296-5p
c+
LG
HG
E
miR-296-5p expression in VSMCs
Fold induction
p=0.06
p=0.002
PDGF-BB
LG
HG
F
miR-296-5p expression in VSMCs
Fold induction
p=0.007
p=0.002
HG-EVs control siRNA
HG-EVs PDGF-BB siRNA
HG

624

Figure 7

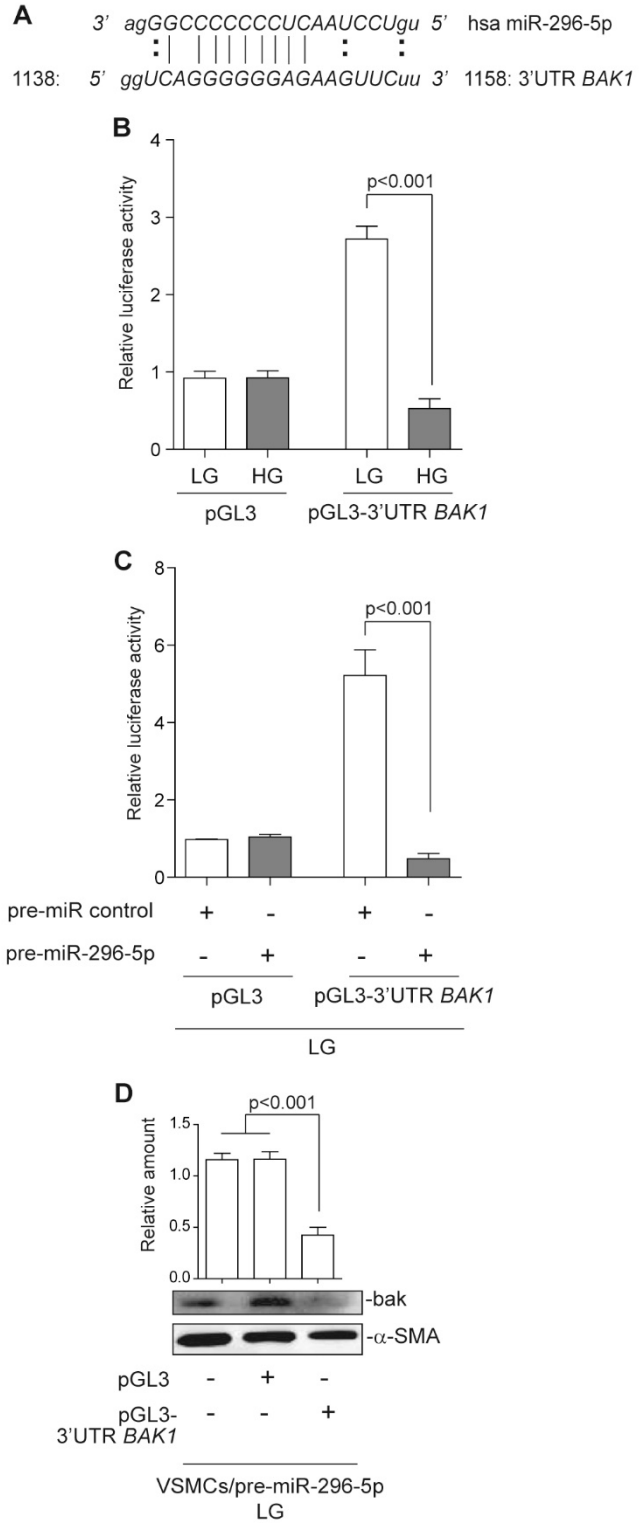
A
3' agGGCCCCCCCUCAAUCCUgu 5' hsa miR-296-5p
1138: 5' ggUCAGGGGGGAGAAGUUCuu 3' 1158: 3'UTR BAK1
B
Relative luciferase activity
p<0.001
LG HG LG HG
pGL3
pGL3-3'UTR BAK1
C
Relative luciferase activity
p<0.001
pre-miR control + - + -
pre-miR-296-5p - + - +
pGL3
pGL3-3'UTR BAK1
LG
D
Relative amount
p<0.001
-bak
-α-SMA
pGL3 - + -
pGL3-3'UTR BAK1 - - +
VSMCs/pre-miR-296-5p
LG

625

Figure 8

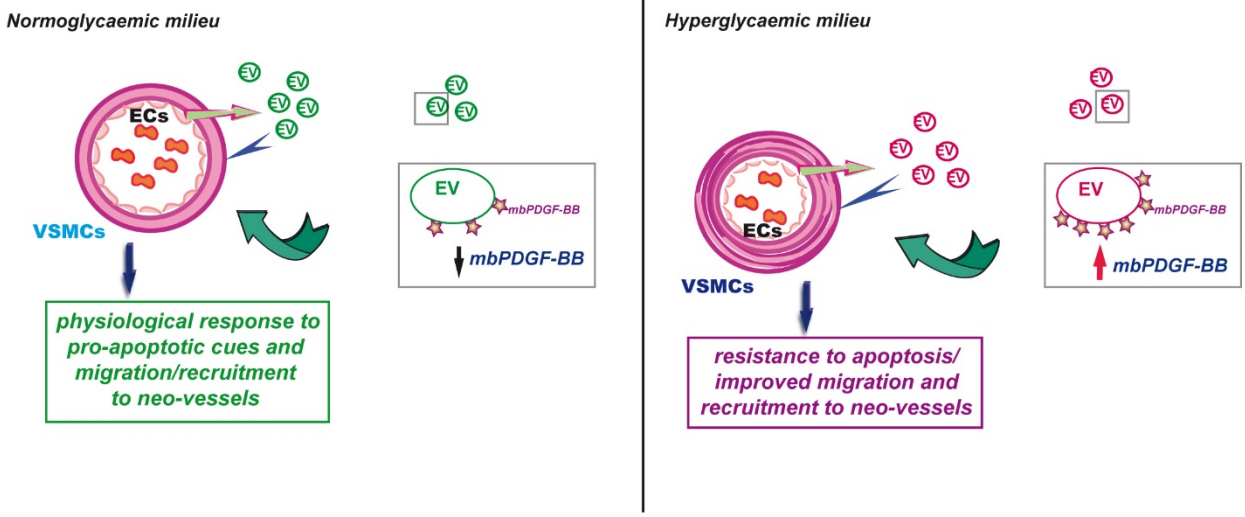
Normoglycaemic milieu
ECs
VSMCs
EV
mbPDGF-BB
physiological response to pro-apoptotic cues and migration/recruitment to neo-vessels
Hyperglycaemic milieu
ECs
VSMCs
EV
mbPDGF-BB
resistance to apoptosis/ improved migration and recruitment to neo-vessels

626